

## K-site splitting in $\text{KTiOPO}_4$ at room temperature

Stefan T. Norberg\* and Nobuo Ishizawa

Ceramics Research Laboratory, Nagoya Institute of Technology, 10-6-29 Asahigaoka, Tajimi, Gifu 507-0071, Japan

Correspondence e-mail: stefan.norberg@gmail.com

Received 31 May 2005

Accepted 24 August 2005

Online 17 September 2005

The room-temperature structure of potassium titanyl phosphate ( $\text{KTiOPO}_4$ , KTP) with  $Pna2_1$  symmetry has been studied by means of synchrotron radiation. Each of the two crystallographically unique K1 and K2 cations is split over two sites that are shifted along the  $c$  direction by 0.287 (13) and 0.255 (13) Å for the K1*a/b* and K2*a/b* pairs, respectively. The refined populations of the minor K1*b* and K2*b* sites are 0.102 (12) and 0.132 (17), respectively. It is shown that accurate high-resolution synchrotron data ( $R_{\text{merged}} = 0.015$  for 25 010 reflections, 9456 unique,  $\sin\theta/\lambda$  limit > 1.0) are required for the determination of a reliable structure model.

### Comment

The  $\text{KTiOPO}_4$  (KTP, potassium titanyl phosphate) structure was determined by Tordjman *et al.* (1974). The highly asymmetric bonds in the non-centrosymmetric structure indicated its potential as a non-linear optical (NLO) material, as later confirmed by Zumsteg *et al.* (1976). Since then, KTP has become one of the best known materials for various NLO applications (Bierlein, 1989; Stucky *et al.*, 1989) and it is the material of choice in applications that utilize the second harmonic generating effect for laser-frequency doubling (Boulanger *et al.*, 1994). The transparent crystalline material has favourable material properties, such as a high thermal stability, chemical stability, high optical non-linearity and a high optical damage threshold. Additionally, the crystals have a wide optical transmission window that covers both the UV and IR spectra. These properties are also found in some isostructural  $\text{ATiOBO}_4$  materials, particularly for those with  $A = \text{K, Rb, Cs or Tl}$  and  $B = \text{P or As}$ .

KTP has a well known structure which, upon heating, undergoes a reversible ferroelectric (space group  $Pna2_1$ ) to paraelectric (space group  $Pnan$ ) phase transition at  $\sim 1207$  K (Stefanovich *et al.*, 1996). The exact temperature depends on variations in growth conditions, such as the K/P ratio in the flux (Angert *et al.*, 1995). Belokoneva *et al.* (1997) have described the temperature-induced phase transition as being both displacive and of an order–disorder nature, unlike the

purely displacive phase transition under high pressure at ambient temperature.

Belokoneva *et al.* (1990) were the first to report on alkali site splitting in KTP isostructures. They refined split sites for the K cations in  $\text{KFeFPO}_4$  and mentioned that a similar phenomenon existed for KTP. However, no details were provided of the data collection or the structural parameters for KTP in either their paper or the Inorganic Crystal Structure Database (ICSD, 2001), except that the minor K split positions have a population of 0.1. The description of alkali hole sites and framework pseudosymmetry for  $\text{KTiOPO}_4$  isostructures was later discussed and improved by Thomas *et al.* (1990) and Thomas & Glazer (1991). More recent investigations relating to the temperature dependence of the K-cation site behaviour were carried out by Delarue *et al.* (1998, 1999) and Norberg and co-workers (Norberg, Sobolev & Streltsov, 2003; Norberg, Gustafsson & Mellander, 2003). The latter studies resulted in a general description of the relationship between the temperature and the structural behaviour of the alkali sites.

The splitting of alkali sites has also been found at room temperature in several KTP isostructures, *e.g.*  $\text{RbTiOAsO}_4$  (Streltsov *et al.*, 2000),  $\text{CsTiOAsO}_4$  (Nordborg, 2000) and  $\text{RbSbOGeO}_4$  (Belokoneva *et al.*, 1997). It has, on the other hand, only been observed in KTP at temperatures of 673 K and above (Delarue *et al.*, 1999). The thorough data collected by Delarue *et al.* at 273, 673 and 973 K revealed the splitting of K sites at both 673 and 973 K but not at 273 K, even though their published residual electron-density maps suggest the presence of splitting. The very detailed structural investigations of KTP at room temperature by Hansen *et al.* (1991) and Dahaoui *et al.* (1997) did not reveal any site splitting either, although these studies were mainly concerned with the charge density in the  $\text{TiO}_6$  octahedra.

We reinvestigated the KTP structure using high-resolution synchrotron data, with the specific purpose of confirming the earlier results reported by Belokoneva *et al.* (1990). In this paper, we report that each of KTP's crystallographically independent K cations is undoubtedly split over two adjacent sites at room temperature. Possible reasons why this has been missed in previous studies of the KTP structure are discussed by analyzing the correlation between the quality of the diffraction data and the details of the refined structure.

The data were refined utilizing the *Xtal3.7* software package (Hall *et al.*, 2000), first as KTP without any K-site splitting and with atomic parameters from Norberg *et al.* (2000) (model I). This model converged to  $R = 0.021$ ,  $wR = 0.027$ ,  $S = 1.078$  and residual electron densities  $\Delta\rho_{\text{max}}/\Delta\rho_{\text{min}}$  of  $1.56/-0.91 \text{ e \AA}^{-3}$  [ $\sigma(\Delta\rho) = 0.09 \text{ e \AA}^{-3}$ ]. The resulting residual electron-density maps were extremely flat and clean of peaks except close to each K site. Peaks of  $1.56$  and  $1.31 \text{ e \AA}^{-3}$  were found  $0.496(1) \text{ \AA}$  from K1 and  $0.474(1) \text{ \AA}$  from K2, respectively, both corresponding to splitting along the  $c$  direction (Figs. 1*a* and *b*). The residual electron-density peaks in model I prompted a second refinement with split K sites (model II). This model converged to  $R = 0.019$ ,  $wR = 0.025$ ,  $S = 0.996$  and residual electron densities  $\Delta\rho_{\text{max}}/\Delta\rho_{\text{min}}$  of  $1.02/-0.64 \text{ e \AA}^{-3}$

$[\sigma(\Delta\rho) = 0.09 \text{ e } \text{\AA}^{-3}]$ . The minor K1*b* and K2*b* sites are located 0.287 (13) and 0.255 (13) Å from the original K1*a* and K2*a* sites, with occupancies of 0.102 (12) and 0.132 (17), respectively. The surrounding residual electron densities are as shown in Figs. 1(c) and (d).

The K1*a* and K1*b* cations occupy slightly smaller cation cages and have rather irregular coordination polyhedra with all shorter K—O bonds roughly parallel to the (001) plane. The K1*a* coordination environment includes four shorter bonds [between 2.7187 (14) and 2.7593 (14) Å] and four longer bonds [between 2.858 (2) and 3.0425 (18) Å]. Cation K1*b* is shifted from K1*a* along the positive *c* direction and is, thus, barely coordinated to six O atoms with four shorter bonds [between 2.657 (7) and 2.764 (7) Å] and two longer bonds [3.034 (10) and 3.122 (14) Å]. Displacement ellipsoid plots of the K1O<sub>*x*</sub> polyhedra are shown in Fig. 2. The K2O<sub>*x*</sub> polyhedra are similar.

Our results confirm the presence of split K sites in KTP at room temperature. Energy-dispersive X-ray analysis did not indicate any contamination by other alkali cations and the coordination environments of the split sites do not correspond to other alkali metals such as Na, for instance, which would require much shorter Na—O bond lengths. The splitting of K sites has also been confirmed by another data collection and structure refinement carried out on a KTP crystal from a different crystal growth experiment. This second refinement [ $R_{\text{int}}$  of 0.042 due to a shorter scan time,  $R = 0.031$ ,  $wR = 0.041$ ,  $S = 1.003$ ,  $\Delta\rho_{\text{max}}/\Delta\rho_{\text{min}}$  of 0.81/−0.66 e Å<sup>−3</sup>,  $\sigma(\Delta\rho) = 0.11 \text{ e } \text{\AA}^{-3}$ ] yielded almost exactly the same structure. The

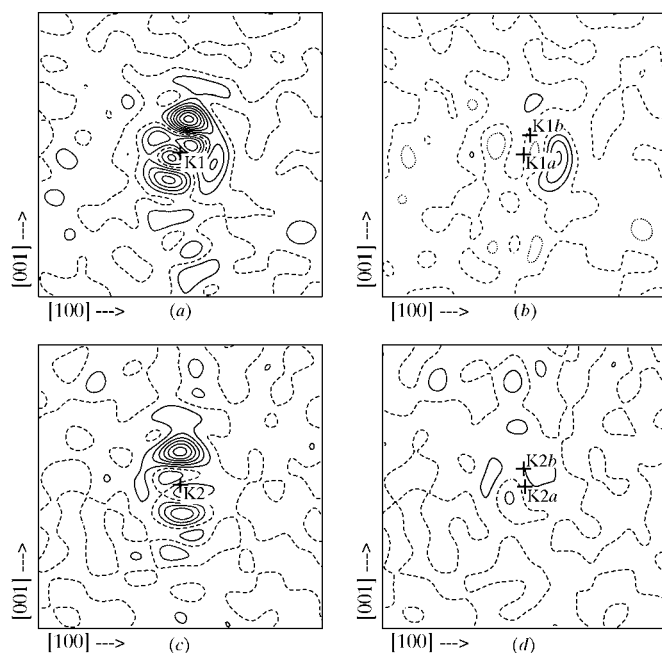


**Figure 1**

$\Delta\rho$  maps in the (010) plane through the K1 and K2 sites for model I with unsplit sites (a, c) and model II with split sites (b, d). Contour intervals are  $0.2 \text{ e } \text{\AA}^{-3}$  [ $\sigma(\Delta\rho) = 0.08 \text{ e } \text{\AA}^{-3}$ ]. The positive and negative contours are shown as solid and short dashed lines, respectively. Map borders are  $4 \times 4 \text{ \AA}$ .

K1*b* site is shifted by 0.266 (16) Å from the K1*a* site with an occupancy of 0.121 (19), and K2*b* is likewise located 0.241 (17) Å from K2*a* with an occupancy of 0.15 (2). All features of the residual electron-density map are also remarkably similar to those in the KTP structure reported in this paper.

It should be noted that an alternative to a split-cation model is an anharmonic model using a Gram–Charlier expansion series for the modelling of thermal displacement parameters. However, Delarue *et al.* (1999) concluded that such a single-site model is not adequate for KTP, and that a more sophisticated model with split K sites, with the distance between the split sites decreasing to zero at 0 K, is needed.

The earlier failures to characterize correctly the K-site splitting in KTP are due to a low resolution or to a lack of intensity in the diffraction data, or a combination of both. KTP isostructures are characterized by a remarkably large number of weak reflections (Streltsov *et al.*, 2000), so studies based on X-ray sealed-tube data will certainly suffer from the low statistical significance of the weak reflections. The effect of limited resolution was investigated in the present work by refining the diffraction data using  $\sin\theta/\lambda$  limits of 0.6, 0.7, 0.8, 0.9 and 1.0, respectively. The results show conclusively that using data with a limited resolution greatly decreases the likelihood of successfully identifying the split K sites (Fig. 3). For instance, a  $\sin\theta/\lambda$  limit of 0.6 ( $2\theta_{\text{max}} = 53.5^\circ$ ) allows the refinement of a structure model with unsplit K sites to a final  $R$  value of 0.011, without any disturbing residual electron-density peaks (Fig. 3a).

The effect of different  $\sin\theta/\lambda$  limits on the refinement of the structure model with unsplit K sites (model I) is shown in Table 2. The significant difference between  $|\Delta\rho_{\text{max}}|$  and  $|\Delta\rho_{\text{min}}|$  appearing around  $\sin\theta/\lambda = 0.7$  suggests the failure of this model. However, these data still do not allow a reliable refinement of the split sites. As described in Table 3, the splitting of K sites (model II) is only correctly refined with a resolution of  $\sin\theta/\lambda = 1.0$  and a higher resolution seems to yield little improvement to the structure model. However, it should be noted that our data are not only of high resolution ( $2\theta_{\text{max}} = 110.02^\circ$ ) but also of good statistical quality, as indi-

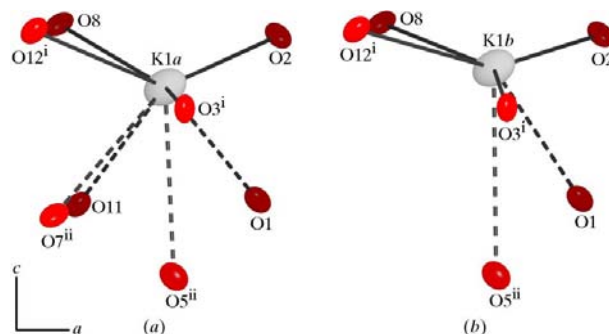


**Figure 2**

(a) The K1*a* and (b) the K1*b* coordination polyhedra, with displacement ellipsoids drawn at the 80% probability level. Symmetry codes are as given in Table 1.

cated by the low  $R_{\text{int}}$  value of 0.015. It is likely, therefore, that data with less accurate statistics will need an even higher resolution for the correct identification of the K-site splitting in KTP.

The recent investigation of split alkali sites in  $\text{RbTiOAsO}_4$  by Streltsov *et al.* (2000) was also carried out by means of synchrotron radiation at room temperature. The  $\text{Rb1a-Rb1b}$  and  $\text{Rb2a-Rb2b}$  distances of 0.312 (3) and 0.233 (4) Å, respectively, are similar to those in the present report. Further investigations of KTP isostructures using synchrotron data are likely to result in more structures with accurately determined alkali site splitting at room temperature. Previous determinations of alkali site splitting might also benefit from reinvestigation, since we have demonstrated the importance of high-resolution synchrotron data for such studies. Finally, it is noteworthy that no charge-density analysis of the KTP structure has taken the splitting of K sites into account, and such structural disorder might be of value to improve current charge-density models.

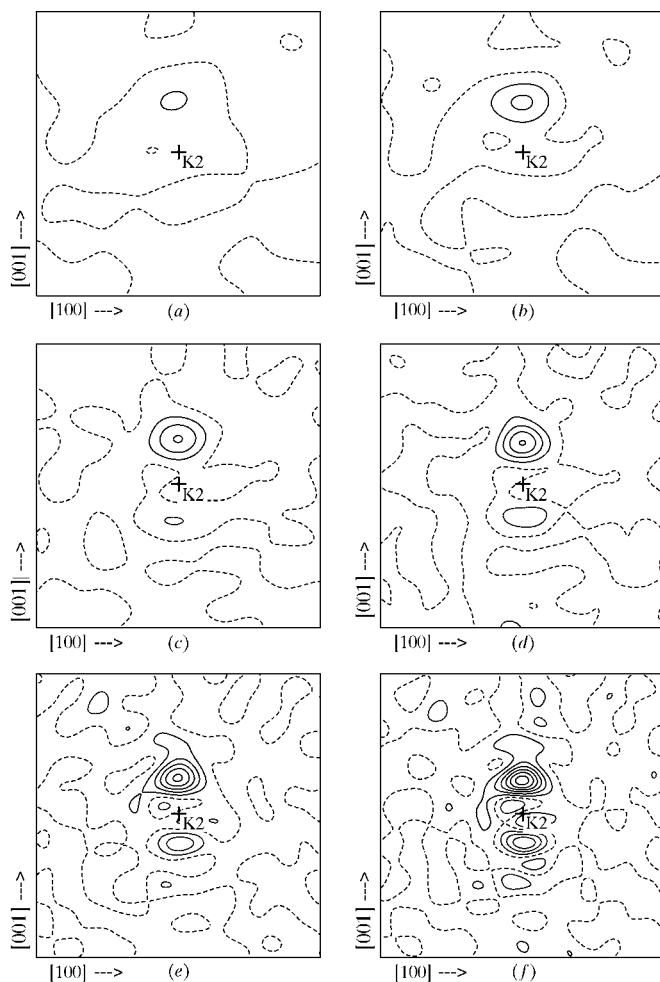


**Figure 3**  
 $\Delta\rho$  maps in the (010) plane through the K2 site refined as model I with  $\sin\theta/\lambda$  limits of 0.6 (a), 0.7 (b), 0.8 (c), 0.9 (d), 1.0 (e) and no limit (f). Contour intervals are  $0.2 \text{ e } \text{Å}^{-3}$  [ $\sigma(\Delta\rho) = 0.08 \text{ e } \text{Å}^{-3}$ ]. The positive and negative contours are shown as solid and short dashed lines, respectively. Map borders are  $4 \times 4 \text{ Å}$ .

## Experimental

Single crystals of KTP were grown by spontaneous nucleation in a self-flux containing  $\text{TiO}_2$ ,  $\text{KH}_2\text{PO}_4$  and  $\text{K}_2\text{HPO}_4$  in a 1:3:2 molar ratio. The chemicals were mixed thoroughly in a 35 ml platinum crucible and heated to 1373 K over a period of 1 d and held at that temperature for 48 h. The temperature was then lowered to 973 K at a rate of  $3.33 \text{ K h}^{-1}$  and then quickly to room temperature. Water was used to dissolve the flux and transparent colourless crystals (from  $\mu\text{m}$  to mm in size) were recovered. Multiple crystals were analysed using an energy-dispersive X-ray spectrometer (Jeol JED-2001 and JSM-6100) and no sample contamination was observed.

### Crystal data

$\text{K}_2\text{O}_{10}\text{P}_2\text{Ti}_2$	Synchrotron radiation
$M_r = 395.88$	$\lambda = 0.75052 (1) \text{ Å}$
Orthorhombic, $Pna2_1$	Cell parameters from 17 reflections
$a = 12.816 (3) \text{ Å}$	$\theta = 27.9\text{--}49.0^\circ$
$b = 6.4045 (5) \text{ Å}$	$\mu = 3.62 \text{ mm}^{-1}$
$c = 10.5889 (8) \text{ Å}$	$T = 295 (2) \text{ K}$
$V = 869.2 (2) \text{ Å}^3$	Rectangular, colourless
$Z = 4$	$0.04 \times 0.04 \times 0.03 \text{ mm}$
$D_x = 3.026 \text{ Mg m}^{-3}$	

### Data collection

BL14a four-circle diffractometer	$R_{\text{int}} = 0.015$
$\omega$ - $2\theta$ scans	$\theta_{\text{max}} = 55.0^\circ$
Absorption correction: analytical (Alcock, 1974)	$h = -27 \rightarrow 27$
$T_{\text{min}} = 0.943$ , $T_{\text{max}} = 0.978$	$k = -13 \rightarrow 9$
25010 measured reflections	$l = -23 \rightarrow 23$
9456 independent reflections	4 standard reflections
9211 reflections with $F > 2\sigma(F)$	every 200 reflections
	intensity decay: none

### Refinement

Refinement on $F$	$\Delta\rho_{\text{max}} = 1.02 (8) \text{ e } \text{Å}^{-3}$
$R[F^2 > 2\sigma(F^2)] = 0.019$	$\Delta\rho_{\text{min}} = -0.64 (8) \text{ e } \text{Å}^{-3}$
$wR(F^2) = 0.025$	Extinction correction: isotropic, Gaussian
$S = 1.02$	Extinction coefficient: $7.4 (4) \times 10^3$
9211 reflections	Absolute structure: Flack (1983), with 4575 Friedel pairs
154 parameters	Flack parameter: 0.426 (11)
$w = 1/[\sigma^2(F) + 0.02(F)^2]$	
$(\Delta/\sigma)_{\text{max}} = 0.001$	

**Table 1**

Selected interatomic distances (Å).

K1a—O1	2.8870 (17)	K2a—O7 <sup>ii</sup>	2.9144 (14)
K1a—O2	2.7495 (13)	K2a—O8 <sup>ii</sup>	3.020 (2)
K1a—O3 <sup>i</sup>	2.7205 (10)	K2a—K2b	0.255 (13)
K1a—O11	2.9751 (17)	K2b—O1 <sup>iii</sup>	2.616 (7)
K1a—O12 <sup>i</sup>	2.7187 (14)	K2b—O2 <sup>ii</sup>	3.129 (10)
K1a—O5 <sup>ii</sup>	2.858 (2)	K2b—O4 <sup>iv</sup>	2.980 (9)
K1a—O7 <sup>ii</sup>	3.0425 (18)	K2b—O11	2.709 (6)
K1a—O8	2.7593 (14)	K2b—O5 <sup>v</sup>	2.819 (6)
K1a—K1b	0.287 (13)	K2b—O7 <sup>ii</sup>	2.893 (6)
K1b—O1	3.034 (10)	K2b—O8 <sup>ii</sup>	3.195 (9)
K1b—O2	2.656 (7)	Ti1—O1	2.1490 (9)
K1b—O3 <sup>i</sup>	2.721 (6)	Ti1—O2 <sup>vi</sup>	1.9585 (9)
K1b—O12 <sup>i</sup>	2.695 (8)	Ti1—O11	1.9770 (8)
K1b—O5 <sup>ii</sup>	3.122 (14)	Ti1—O12 <sup>ii</sup>	1.7212 (9)
K1b—O8	2.764 (7)	Ti1—O5 <sup>vii</sup>	2.0463 (8)
K2a—O1 <sup>iii</sup>	2.6876 (16)	Ti1—O6 <sup>vii</sup>	1.9900 (8)
K2a—O2 <sup>ii</sup>	2.957 (2)	Ti2—O3	2.0402 (9)
K2a—O3 <sup>ii</sup>	3.013 (3)	Ti2—O4 <sup>iv</sup>	1.9810 (9)
K2a—O4 <sup>iv</sup>	3.141 (2)	Ti2—O11	1.7440 (9)
K2a—O11	2.7703 (15)	Ti2—O12	2.0919 (9)
K2a—O12 <sup>ii</sup>	3.034 (2)	Ti2—O7 <sup>vii</sup>	1.9704 (9)
K2a—O5 <sup>v</sup>	2.8049 (13)	Ti2—O8	1.9902 (9)

Symmetry codes: (i)  $x, y - 1, z$ ; (ii)  $-x + \frac{1}{2}, y - \frac{1}{2}, z - \frac{1}{2}$ ; (iii)  $x - \frac{1}{2}, -y + \frac{1}{2}, z$ ; (iv)  $x - \frac{1}{2}, -y + \frac{3}{2}, z$ ; (v)  $-x, -y + 1, z - \frac{1}{2}$ ; (vi)  $-x + 1, -y + 1, z - \frac{1}{2}$ ; (vii)  $-x + \frac{1}{2}, y + \frac{1}{2}, z - \frac{1}{2}$ .

**Table 2**

Refinement of model I as a function of the  $\sin\theta/\lambda$  limit.

$\sin\theta/\lambda$ limit	$R_{\text{int}}$	$R$	$R_w$	GoF	$\Delta\rho_{\text{max}}/\Delta\rho_{\text{min}}$ ( $\text{e}\ \text{\AA}^{-3}$ )
0.6	0.011	0.011	0.017	1.05	0.25 (2) / -0.24 (2)
0.7	0.012	0.012	0.017	0.97	0.44 (3) / -0.26 (3)
0.8	0.013	0.013	0.018	0.95	0.66 (4) / -0.39 (4)
0.9	0.014	0.015	0.021	0.98	0.82 (5) / -0.52 (5)
1.0	0.015	0.018	0.024	1.04	1.13 (7) / -0.77 (7)
None	0.015	0.021	0.027	1.08	1.56 (9) / -0.91 (9)

**Table 3**

Refinement of the K-site splitting in model II as a function of the  $\sin\theta/\lambda$  limit.

$\sin\theta/\lambda$ limit	K1b occupancy	K1b–K1a ( $\text{\AA}$ )	K2b occupancy	K2b–K2a
0.6	0.03 (3)	0.44 (13)	0.07 (6)	0.34 (10)
0.7	0.06 (3)	0.35 (5)	0.08 (4)	0.31 (5)
0.8	0.070 (17)	0.33 (3)	0.09 (3)	0.30 (3)
0.9	0.075 (13)	0.33 (2)	0.088 (19)	0.29 (3)
1.0	0.096 (13)	0.295 (15)	0.115 (19)	0.267 (17)
None	0.102 (12)	0.287 (13)	0.132 (17)	0.255 (13)

A small transparent crystal, with KTP morphology as described by Bolt & Bennema (1990), was used for the data collection at Photon Factory, Tsukuba, Japan, using the beamline 14A four-circle diffractometer (Satow & Iitaka, 1989). Vertically polarized X-ray radiation from a vertical wiggler was monochromated by a double Si(111) perfect crystal monochromator, and focused using a curved fused-quartz mirror coated with platinum. The beam optics are automatically adjusted every 20 min for maximum flux. A high-speed avalanche photodiode detector with counting linearity up to  $10^8$  counts per second was used (Kishimoto *et al.*, 1998). The experimental set-up was similar to that described by Streltsov *et al.* (1998). Diffraction intensities were measured at room temperature with  $\lambda = 0.75052$  (1)  $\text{\AA}$  using  $\omega/2\theta$  continuous time scans with an  $\omega$ -scan width of  $0.30^\circ$ . The collected X-ray intensities were corrected for experimental intensity variations as indicated by measured standard reflections, and for absorption using an analytical model (Alcock, 1974). Anomalous scattering factors were taken from Sasaki (1989) and the linear absorption coefficient  $\mu$  was calculated using mass attenuation coefficients for neutral atoms at 0.75  $\text{\AA}$  (Sasaki, 1990). An isotropic extinction parameter (Zachariassen, 1967) using Larson's implementation (Larson, 1970) was refined for both models and about 1.3% of the reflections were affected by extinction. The maximum correction of  $y = 0.94$  was used for the 800 reflection (the observed structure factor is  $F_{\text{obs}} = yF_{\text{kin}}$ , where  $F_{\text{kin}}$  is the kinematic value). The Flack (1983) parameter refined to 0.426 (1) for both models, indicating that the crystal contained a mixture of domains with opposite polarization. As commonly observed in other KTP-related structures, the low-temperature  $Pna2_1$  structure of  $\text{KTiOPO}_4$  deviates only slightly from the high-temperature centrosymmetric  $Pnan$  structure, the largest atomic displacements being equal to approximately 0.66  $\text{\AA}$  for the alkali cations. Nevertheless, the deviations are significant and the non-centrosymmetric structure model is the only one consistent with the known physical properties of KTP.

Data collection: *DIFF14A* (Vaalsta & Hester, 1997); cell refinement: *LATCON* in *Xtal3.7* (Hall *et al.*, 2000); data reduction: *DIFDAT*, *ADDREF*, *SORTRF* and *ABSORB* in *Xtal3.7*; program(s) used to solve structure: atomic parameters from Norberg *et al.* (2000); program(s) used to refine structure: *CRYLSQ* in *Xtal3.7*; molecular

graphics: *DIAMOND* (Brandenburg, 2001), and *FOURR*, *SLANT* and *CONTRS* in *Xtal3.7*; software used to prepare material for publication: *BONDLA*, *ATABLE* and *CIFIO* in *Xtal3.7*.

Mr Hisashi Hibino is thanked for help with the energy-dispersive X-ray diffraction measurement. SN acknowledges a JSPS postdoctoral fellowship (No. P03707). This study was part of a synchrotron radiation experiment (No. 2004 G048) carried out at the Photon Factory, Tsukuba, Japan.

Supplementary data for this paper are available from the IUCr electronic archives (Reference: BC1075). Services for accessing these data are described at the back of the journal.

## References

- Alcock, N. W. (1974). *Acta Cryst.* **A30**, 332–335.
- Angert, N., Tseitlin, M., Yashchin, E. & Roth, M. (1995). *Appl. Phys. Lett.* **67**, 1941–1943.
- Belokoneva, E. L., Knight, K. S., David, W. I. F. & Mill, B. V. (1997). *J. Phys. Condens. Matter*, **9**, 3833–3851.
- Belokoneva, E. L., Yakubovich, O. V., Tsirelson, V. G. & Urusov, V. S. (1990). *Izv. Akad. Nauk SSSR Neorg. Mater.* **26**, 595–601.
- Bierlein, J. D. (1989). *SPIE Int. Soc. Opt. Eng.* **1104**, 2–11.
- Bolt, R. J. & Bennema, P. (1990). *J. Cryst. Growth*, **102**, 329–340.
- Boulanger, B., Feve, J. P., Marnier, G., Menaert, B., Cabirol, X., Villeval, P. & Bonnin, C. (1994). *J. Opt. Soc. Am. B*, **11**, 750–757.
- Brandenburg, K. (2001). *DIAMOND*. Release 2.1e. Crystal Impact GbR, Bonn, Germany.
- Dahaoui, S., Hansen, N. K. & Menaert, B. (1997). *Acta Cryst.* **C53**, 1173–1176.
- Delarue, P., Lecomte, C., Jannin, M., Marnier, G. & Menaert, B. (1998). *Phys. Rev. B*, **58**, 5287–5295.
- Delarue, P., Lecomte, C., Jannin, M., Marnier, G. & Menaert, B. (1999). *J. Phys. Condens. Matter*, **11**, 4123–4134.
- Flack, H. D. (1983). *Acta Cryst.* **A39**, 876–881.
- Hall, S. R., du Boulay, D. J. & Olthof-Hazekamp, R. (2000). Editors. *Xtal3.7 Reference Manual*. University of Western Australia: Lamb, Perth.
- Hansen, N. K., Protas, J. & Marnier, G. (1991). *Acta Cryst.* **B47**, 660–672.
- ICSD (2001). Inorganic Crystal Structure Database. Version 2004-2. FIZ-Karlsruhe. URL: <http://www.fiz.karlsruhe.de/fiz/products/icsd/welcome.html>.
- Kishimoto, S., Ishizawa, N. & Vaalsta, T. P. (1998). *Rev. Sci. Instrum.* **69**, 384–391.
- Larson, A. C. (1970). *Crystallographic Computing*, edited by F. R. Ahmed, S. R. Hall & C. P. Huber, pp. 291–294. Copenhagen: Munksgaard.
- Norberg, S. T., Gustafsson, J. & Mellander, B.-E. (2003). *Acta Cryst.* **B59**, 588–595.
- Norberg, S. T., Sobolev, A. N. & Streltsov, V. A. (2003). *Acta Cryst.* **B59**, 353–360.
- Norberg, S. T., Streltsov, V. A., Svensson, G. & Albertsson, J. (2000). *Acta Cryst.* **B56**, 980–987.
- Nordborg, J. (2000). *Acta Cryst.* **C56**, 518–520.
- Sasaki, S. (1989). *Numerical Tables of Anomalous Scattering Factors Calculated by the Cromer and Mann's Method*. KEK Report 88-14, pp. 1–136.
- Sasaki, S. (1990). *X-ray Absorption Coefficients for the Elements (Li to Bi, U)*. KEK Report 90-16, pp. 1–143.
- Satow, Y. & Iitaka, Y. (1989). *Rev. Sci. Instrum.* **60**, 2390–2393.
- Stefanovich, S., Mosunov, A., Mill, B. & Belokoneva, E. (1996). *Ferroelectrics*, **185**, 63–66.
- Streltsov, V. A., Ishizawa, N. & Kishimoto, S. (1998). *J. Synchrotron Rad.* **5**, 1309–1316.
- Streltsov, V. A., Nordborg, J. & Albertsson, J. (2000). *Acta Cryst.* **B56**, 785–792.
- Stucky, G. D., Phillips, M. L. F. & Gier, T. E. (1989). *Chem. Mater.* **1**, 492–509.
- Thomas, P. A. & Glazer, A. M. (1991). *J. Appl. Cryst.* **24**, 968–971.
- Thomas, P. A., Glazer, A. M. & Watts, B. E. (1990). *Acta Cryst.* **B46**, 333–343.
- Tordjman, I., Masse, R. & Guitel, J. C. (1974). *Z. Kristallogr.* **139**, 103–115.
- Vaalsta, T. P. & Hester, J. R. (1997). *DIFF14A*. Photon Factory, Tsukuba, Japan.
- Zachariassen, W. H. (1967). *Acta Cryst.* **23**, 558–564.
- Zumsteg, F. C., Bierlein, J. D. & Gier, T. E. (1976). *J. Appl. Phys.* **47**, 4980–4985.